



OPEN ACCESS

EDITED BY
Shuren Wang,
Henan Polytechnic University, China

REVIEWED BY
Pengfei Shan,
Xi'an University of Science and
Technology, China
Jianwei Cheng,
China University of Mining and
Technology, China

*CORRESPONDENCE
Huaibin Li,
LHB_aust@126.com

SPECIALTY SECTION
This article was submitted to
Geohazards and Georisks,
a section of the journal
Frontiers in Earth Science

RECEIVED 21 August 2022
ACCEPTED 12 September 2022
PUBLISHED 28 September 2022

CITATION
Li H, Zhao X, Dai B, Huang Z and Zhu Q
(2022), Study on the evolution and
prediction of fracture depth of
surrounding rock in deep mining
roadway based on numerical analysis
and borehole detection.
Front. Earth Sci. 10:1024240.
doi: 10.3389/feart.2022.1024240

COPYRIGHT
© 2022 Li, Zhao, Dai, Huang and Zhu.
This is an open-access article
distributed under the terms of the
[Creative Commons Attribution License
\(CC BY\)](https://creativecommons.org/licenses/by/4.0/). The use, distribution or
reproduction in other forums is
permitted, provided the original
author(s) and the copyright owner(s) are
credited and that the original
publication in this journal is cited, in
accordance with accepted academic
practice. No use, distribution or
reproduction is permitted which does
not comply with these terms.

Study on the evolution and prediction of fracture depth of surrounding rock in deep mining roadway based on numerical analysis and borehole detection

Huaibin Li^{1,2*}, Xingdong Zhao³, Bibo Dai², Zujun Huang⁴ and Qiankun Zhu³

¹School of Safety Science and Engineering, Anhui University of Science and Technology, Huainan, China, ²State Key Laboratory of Safety and Health for Metal Mines, Maanshan, China, ³Laboratory for Safe Mining in Deep Metal Mine, Northeastern University, Shenyang, China, ⁴Zhuxianzhuang Coal Mine of Huaibei Mining (Group) Co., Ltd., Suzhou, China

The failure of surrounding rock in deep hard rock roadway is closely related to mining disturbance. In this study, the 13# stope ramp of -767 m level (at a buried depth of 1,197 m) at Hongtoushan copper mine was taken as the engineering background, a comprehensive analysis method of numerical analysis and borehole detection was put forward, and the evolution law of fracture depth of the ramp surrounding rock under the mining influence was obtained. The results show that the maximum tangential stress and fracture depth of the ramp surrounding rock on both sidewalls increase slowly at the initial mining stage. When the ore body above the ramp is mined, the maximum tangential stress and fracture depth of the ramp surrounding rock on both sidewalls increase rapidly, and the two parameters are positively correlated. Based on this, the ratio of the maximum tangential stress of the surrounding rock to the uniaxial compressive strength of intact rock ($\sigma_{\theta\max}/\sigma_c$) and the equivalent radius (a) of the roadway were used as parameters, and an equation for the fracture depth of the roadway surrounding rock was proposed. Through the case analysis, the results show that the proposed equation of fracture depth of the roadway surrounding rock has good prediction accuracy. This study enriches the research on the stability and failure mechanism of the roadway surrounding rock under the mining disturbance, and provides new basis for the support design of mining roadways.

KEYWORDS

ramp, mining influence, numerical analysis, borehole detection, fracture depth equation

Introduction

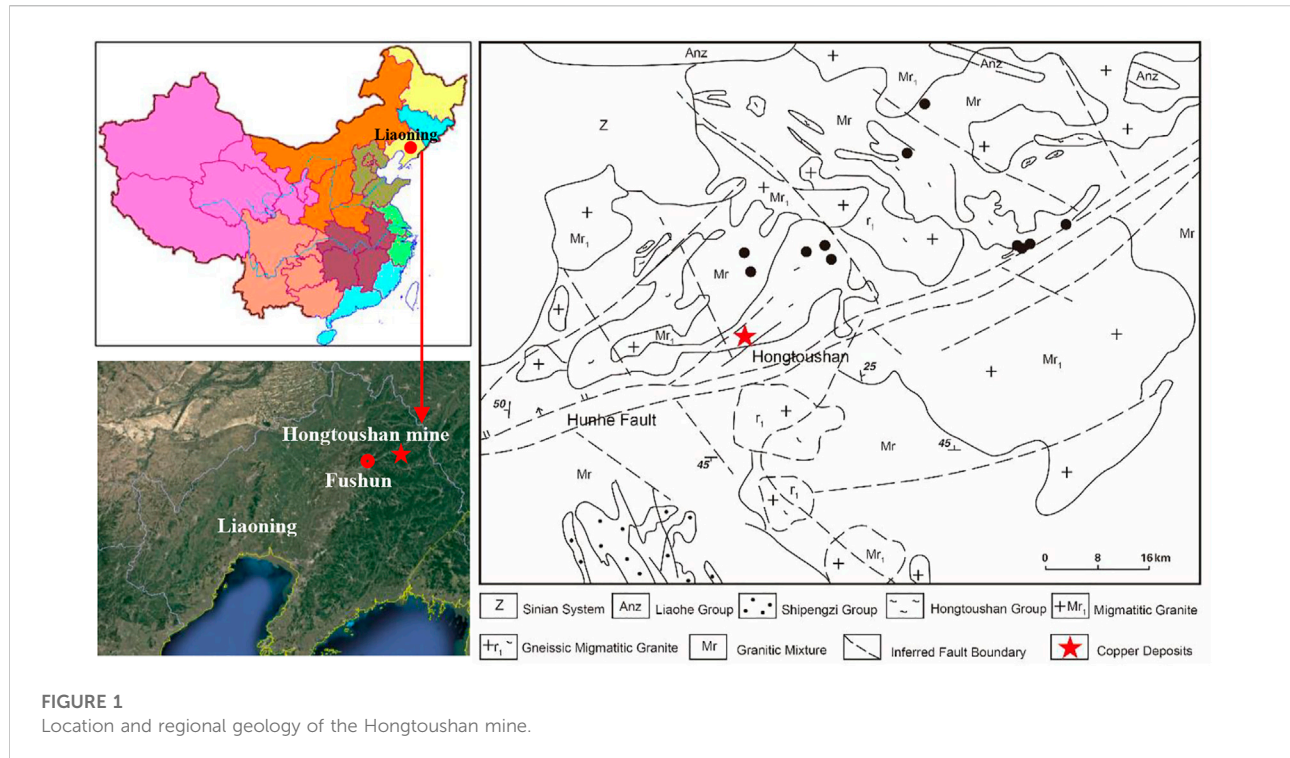
The overhand cut-and-fill mining method has been widely used in deep metal deposits, and the transportation roadway has generally been arranged at the footwall of the ore body. The deep stope and the roadway surrounding rock are often in a complex stress environment (i.e., high ground stress, high ground temperature, high osmotic pressure, and strong mining disturbance). When the mining stress is greater than the strength of the surrounding rock of the stope (roadway), the spalling, rockburst and other failures of the surrounding rock can be induced easily. As a result, the ore loss and dilution, equipment damage and personnel casualties can be caused, which seriously hinders the normal production of the mine (Read, 2004; Zhao et al., 2013; Abdellah et al., 2014; Zheng et al., 2015; Wei et al., 2022).

At present, research on the failure of the surrounding rock of stope (roadway) induced by deep mining has been widely conducted, and some progress in the mechanics and mining engineering has been obtained. Through borehole television monitoring and acoustic testing, Wang et al. (2015) studied the damage range of roadway surrounding rock, and concluded that the damage range of the roadway surrounding rock under the mining influence is larger than that without mining influence. Based on the numerical simulation method, Zhang and Mitri (2008) explored the key factors affecting the plastic zone of the surrounding rock in the footwall transport roadway. It was found that under the mining influence, the plastic zone of the surrounding rock of the footwall transport roadway increases with the increase of the buried depth of the roadway, and it also increases with the decrease of the distance between roadway and stope. Through the numerical simulation method, Jia et al. (2017) studied the mechanical mechanism and distribution characteristics of the plastic zone of roadway surrounding rock under the non-uniform stress field. The results showed that when the stress around the roadway is greater than the strength of the surrounding rock and the ratio of principal stress around the roadway is large, the shear failure occurs in the surrounding rock, and a butterfly-shaped plastic zone can be formed. Abdellah et al. (2011) evaluated the issue of haulage drift safety in mining activities using probabilistic methods. Aiming at the Linglong gold mine in China, Cai and Lai (2003) investigated the main influencing factors of the stability of the transport roadway by the coupled data mining techniques, and analyzed the acoustic emission signals and monitoring results. Liu et al. (2019) simulated coal seams with different dip angles through the FALC^{3D} software, and discussed the characteristics of floor failure under the mining influence. Waclawik et al. (2017) monitored the stress of the surrounding rock of the roadway under long-wall mining. It was concluded that the stress of surrounding rock changes with the advance of the working face.

The stress change of the surrounding rock in underground engineering is closely related to rock failure. Researchers have conducted many studies on the relationship between stress and

failure of surrounding rock in engineering. Based on the damage situation of the gold mine in South Africa, Ortlepp and Stacey (1994), Ortlepp (2000) divided the damage degree of the roadway by using the ratio of the maximum principal stress to the uniaxial compressive strength. Specifically, when the maximum principal stress is equal to $0.2\sigma_f$, the spalling failure occurs in the surrounding rock, when it exceeds $0.4\sigma_f$, rockburst occurs in the surrounding rock. By using maximum principal stress, minimum principal stress and peak strength σ_f , Wagner and Wiseman (1980) proposed a concept of stress concentration factor. It is concluded that when the stress concentration factor SF is equal to or greater than 0.8, the spalling failure occurs in the roadway surrounding rock. Hoek and Brown (1980) made a more detailed classification of the damage degree of the roadway by using the ratio of the maximum tangential stress of surrounding rock to the uniaxial compressive strength of rock ($\sigma_{\theta\max}/\sigma_c$). When $\sigma_{\theta\max}/\sigma_c$ is equal to 0.34, slight spalling failure occurs in the surrounding rock, when $\sigma_{\theta\max}/\sigma_c$ is equal to 0.42, severe spalling failure occurs in the surrounding rock. Dowding and Andersson (1986) analyzed five typical cases of spalling failure of surrounding rock in tunnels. It is believed that when the ratio of the maximum tangential stress of surrounding rock caused by tunnel excavation to the uniaxial compressive strength of rock ($\sigma_{\theta\max}/\sigma_c$) exceeds 0.35, the spalling failure of surrounding rock occurs, when $\sigma_{\theta\max}/\sigma_c$ exceeds 0.5, the weak or medium rockburst occurs in surrounding rock, when $\sigma_{\theta\max}/\sigma_c$ exceeds 1.0, the strong rock burst occurs in surrounding rock. Based on field-measured data, Martin (1993), Martini et al. (1997), and MartinChristiansson (2009) and Diederichs (2007) fitted empirical formulas with stress intensity ratio and roadway size as parameters, and calculated the fracture depth of the roadway surrounding rock. Perras and Diederichs (2016) predicted the excavation damage zones of the brittle surrounding rock of the underground tunnel by the empirical method and numerical simulation method. Cai and Kaiser (2014) employed numerical simulation and field comparison methods to study the spalling failure strength at the excavation boundary in the field. The results showed that the spalling strength of rock mass at the project site is not 0.4 ± 0.1 times of the uniaxial compressive strength of rock, but generally 0.8 ± 0.05 times of the uniaxial compressive strength of rock. The above research results provide a valuable reference for analyzing the stress, displacement and distribution characteristics of the failure zone of the roadway surrounding rocks under the mining influence. However, there are few studies on the evolution and prediction of the fracture depth of roadway surrounding rock under the influence of deep mining.

The 13# stope ramp of -767 m level (at a buried depth of 1,197 m) at Hongtoushan copper mine, a wide range of spalling failures under the mining influence occurred. Based on this engineering background, the failure mechanism of the ramp surrounding rock was analyzed, and the evolution process of the maximum tangential stress of the ramp surrounding rock during the overhand cut-and-fill mining was obtained by the FLAC^{3D} software. Besides, the fracture depth of the surrounding rock was measured by the borehole detection, the stress-fracture depth evolution process of



surrounding rock under the mining influence was comprehensively analyzed, and the equation of rock fracture depth of mining roadway was proposed by using the ratio of the maximum tangential stress of surrounding rock of the roadway to the uniaxial compressive strength of the intact rock ($\sigma_{\theta, \max}/\sigma_c$) and the equivalent radius (a) of the roadway. This study provides a basis for supporting design and judgment of the fracture depth of roadway surrounding rock under the mining influence.

Site description

Engineering geology

Hongtoushan copper mine is located in the northeast of Liaoning Province, China (Figure 1). At present, it is one of the deepest non-ferrous metal mine in China, with an exploration depth of 1,657 m and a mining depth of 1,257 m. In this mine, the overhand cut-and-fill mining method was adopted. The 13# stope ramp of -767 m level (at a buried depth of 1,197 m) had a stage height of 60 m, a strike length of 50 m, and a stope span of 30 m, and the dip of the stope is 70°. Parallel blast hole rings were fired at a 3 m extracting height in the horizontal panel and using multiple ring sequences. The stope is backfilled with tailings and cement after every slice mined. Access to cut-and-fill stopes is through ramp located in footwall of each stope and inclined at the same dip as the ore body. The horizontal distance between the ramp and 13# stope is about 20 m. The

horse-shoe-shaped ramp is a cross-section of 3.0 m width and 2.8 m height. To obtain the distribution of the structural planes in the stope and surrounding rock, the on-site engineering geological survey of the hanging wall, footwall and ore body of the stope was carried out by using the scan line method. The rock samples were taken on-site and the rock mechanical experiments were carried out. The quality of the surrounding rock of the stope was classified by rock mass rating (RMR) and rock mass quality (Q) methods. The results showed that the quality of rock mass was generally good. The mechanical parameters of the ramp surrounding rock were estimated based on the Hoke-Brown strength criterion, as shown in Table 1.

The regression equations of the maximum horizontal principal stress, minimum horizontal principal stress and vertical stress are obtained by hollow inclusion stress relief method in the field as follows (Zhao et al., 2019).

$$\begin{cases} \sigma_{h, \max} = 0.0273H - 0.5071 \\ \sigma_{h, \min} = 0.0235H - 3.7780 \\ \sigma_v = 0.0316H - 5.6280 \end{cases} \quad (1)$$

where $\sigma_{h, \max}$, $\sigma_{h, \min}$, and σ_v (MPa) are the maximum horizontal principal stress, minimum horizontal principal stress, and vertical principal stress, and H is the depth (m). According to Eq. 1, the maximum horizontal principal stress $\sigma_{h, \max}$ at -767 m (at a buried depth of 1,197 m) reaches 32.2 MPa with a direction of NW, the minor horizontal principal stress $\sigma_{h, \min}$ is 24.4 MPa in the 167°/60° plane, and the vertical principal stress σ_v is 32.2 MPa.

TABLE 1 Mechanical parameters of rock samples and rock mass.

Site	Rock samples				Rock mass		
	Density/kg m ⁻³	Uniaxial compression strength/MPa	Tensile strength/MPa	Young's modulus/GPa	Uniaxial compression strength/MPa	Tensile strength/MPa	Young's modulus/GPa
Hanging wall	2,714	112.30	6.77	50.60	17.56	0.104	12.00
Ore body	4,224	105.50	7.23	55.20	24.80	0.142	15.69
Foot wall	2,724	132.80	7.49	51.00	36.13	0.402	28.40
Backfill	2,251	2.51	0.53	1.50	2.51	0.051	1.50



FIGURE 2
Spalling failure of the ramp surrounding rock in the 13# stope.

Failure mechanism of the ramp surrounding rock

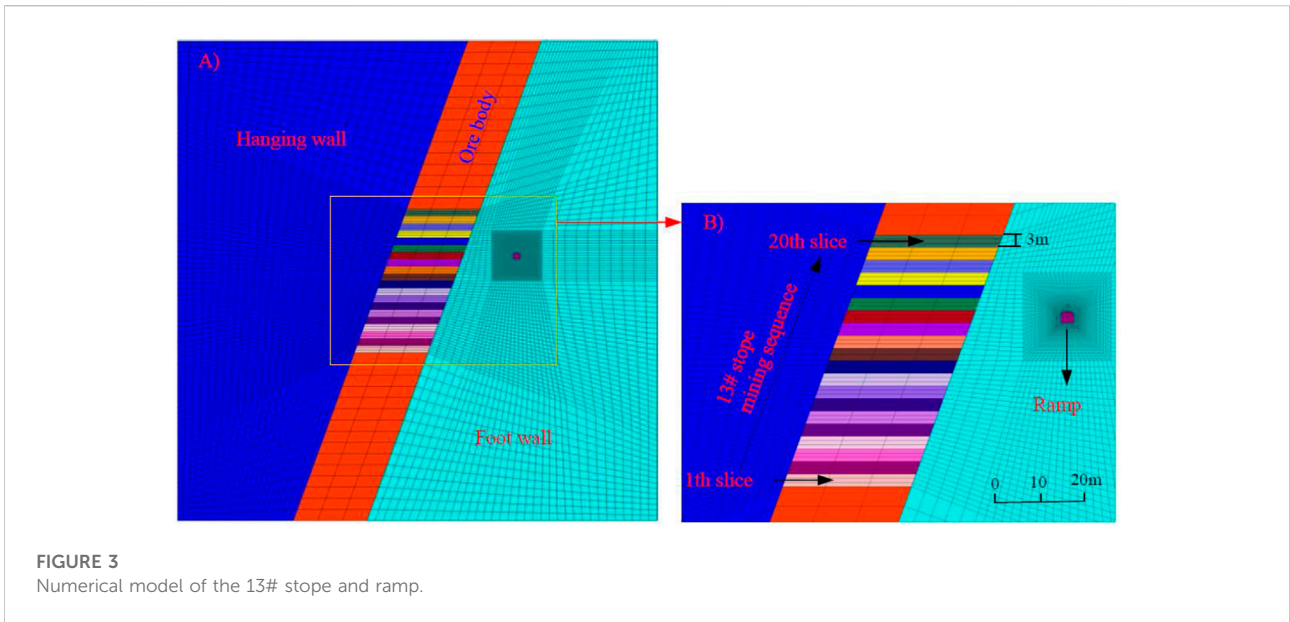
The ramp of 13# stope was arranged in the hard rock mass of the footwall. Due to its large buried depth and close distance to the stope, this ramp was seriously affected by mining. Figure 2 shows the typical spalling failure of the 13# stope ramp under the mining influence. The ramp excavation breaks the balance of the initial stress field, the stress begins to redistribute, the tangential stress of the ramp surrounding rock increases, the radial stress decreases. As a result, the ramp is in a bidirectional stress state. Under the mining influence, the ramp surrounding rock undergoes several stress adjustments. When the maximum tangential stress in surrounding rock exceeds the strength of the rock mass, the stress-induced brittle failure of surrounding rock can be caused. As it is difficult to obtain the strength of rock mass on-site, Hoek and Brown (1980), Dowding and Andersson (1986), Martin et al. (1999), Cai and Kaiser (2014), and Wang et al. (2012) took the ratio of the maximum tangential stress $\sigma_{\theta_{\max}}$ to the uniaxial compressive strength σ_c of intact rock as

the basis of brittle failure of hard rock. It can be seen that the brittle failure of hard rock can be described by $\sigma_{\theta_{\max}}/\sigma_c$. Based on the empirical relationship between $\sigma_{\theta_{\max}}/\sigma_c$ and fracture depth, the maximum tangential stress of the surrounding rock under the mining influence can be obtained by numerical calculation, and the fracture depth of the surrounding rock of the mining roadway can be quickly calculated with the empirical formula. This equation can provide a reference for the support design.

Analysis method for fracture evolution process of the ramp surrounding rock under the mining influence

Numerical analysis

According to the engineering geological conditions of the 13# stope ramp of -767 m level (at a buried depth of 1,197 m),

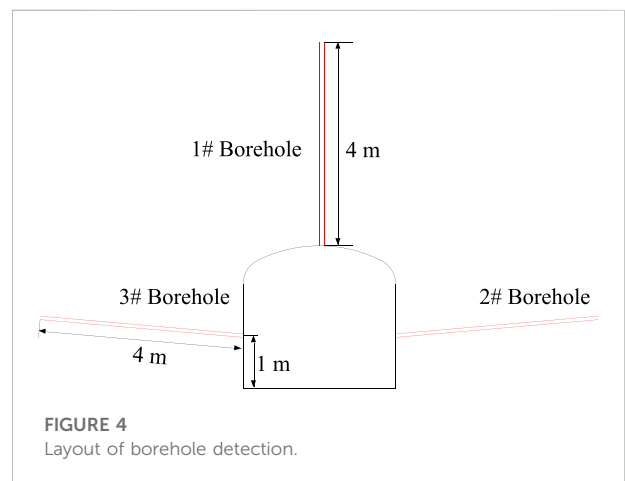


a numerical simulation model was established. It was assumed that the calculation model was a plane strain model, and the rock mass was homogeneous and isotropic. The size of the model was 200 m × 200 m (width × high), and the model was divided into 87,520 units, as shown in Figure 3. To ensure the calculation accuracy, the grid at the ramp position was encrypted. The dip angle of the ore body was 70° and the thickness was 30 m. The mixed boundary conditions were adopted in the model. The vertical and horizontal displacements were restricted on both sidewalls and the bottom of the model. Stress constraints were applied on both sidewalls and the top of the model, and the linear-elastic model was used for simulation.

The FLAC^{3D} software was used to analyze the evolution process of the tangential stress of the ramp surrounding rock of the stope under the mining influence. During the model calculation, the ramp was excavated first, and then the 13# stope was mined from the bottom to the top layers by layers. There were 20 layers in total, and each layer was 3 m high. After the stress balance was reached after the mining of the previous layer, the backfilling of the next layer was conducted.

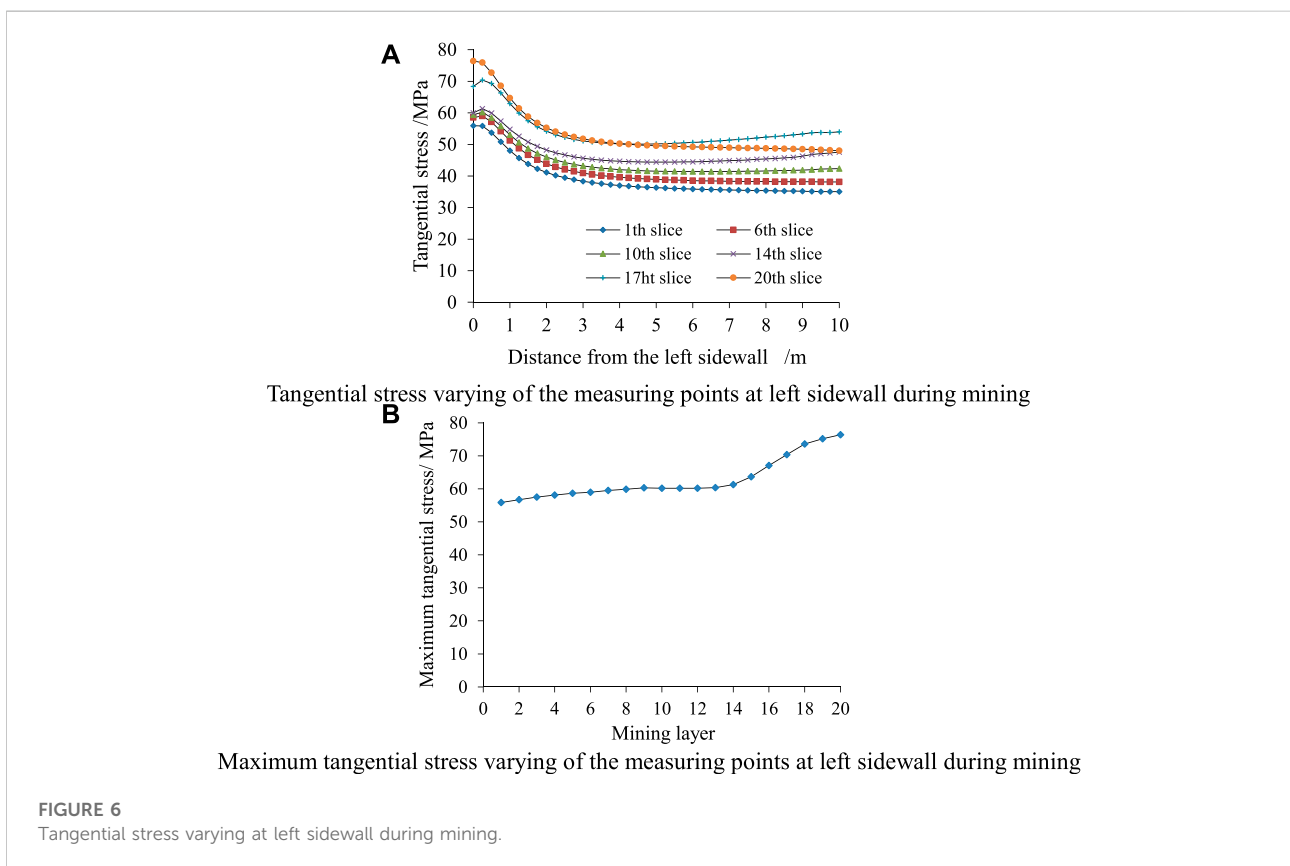
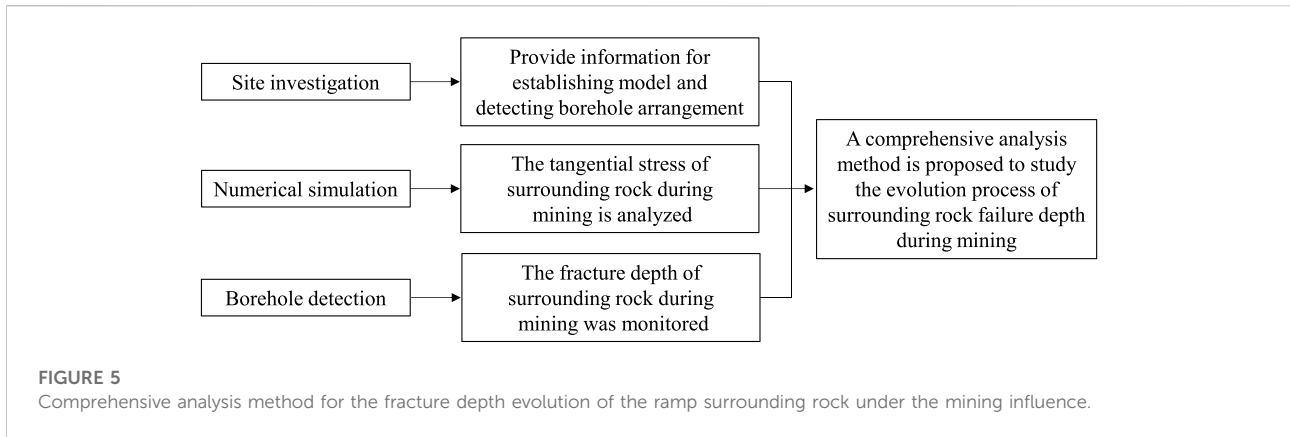
Borehole detection

Borehole detection technology is an intuitive detection method, which can quickly and accurately identify the development of cracks in surrounding rock. At present, the borehole detection method has been rarely used to observe the failure evolution process of the roadway surrounding rock under the deep mining influence in the existing studies. It is



necessary to use the borehole detection method to further reveal the mining-induced failure evolution of roadway surrounding rock.

The ZKXG100-type borehole camera detection device was used on site to detect the fracture depth of the ramp surrounding rock in the 13# stope. Three detection boreholes with a depth of 4 m and a diameter of 40 mm were drilled on the both sidewalls and roof of the ramp. The both sidewalls of the detection boreholes were 1 m high from the floor, with an upward horizontal inclination of 5°. The roof detection boreholes were set perpendicular to the roof. Figure 4 shows the specific layout of the borehole detection. The field observation is from the first layer mining until the end of the 13# stope mining. When mining the ore body below the 14th layer in the 13# stope, the cracks in

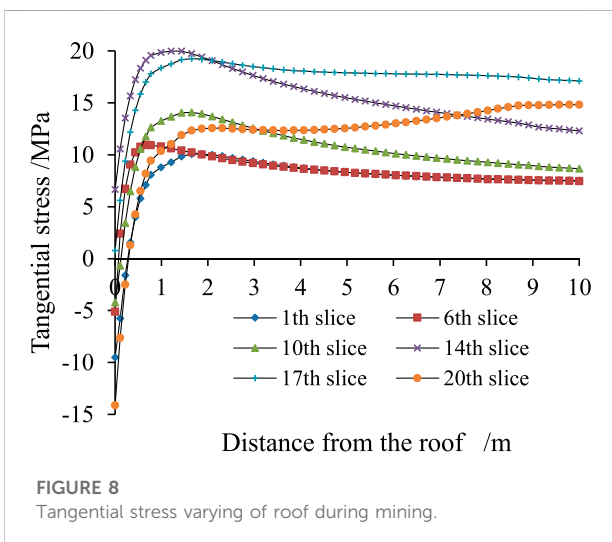
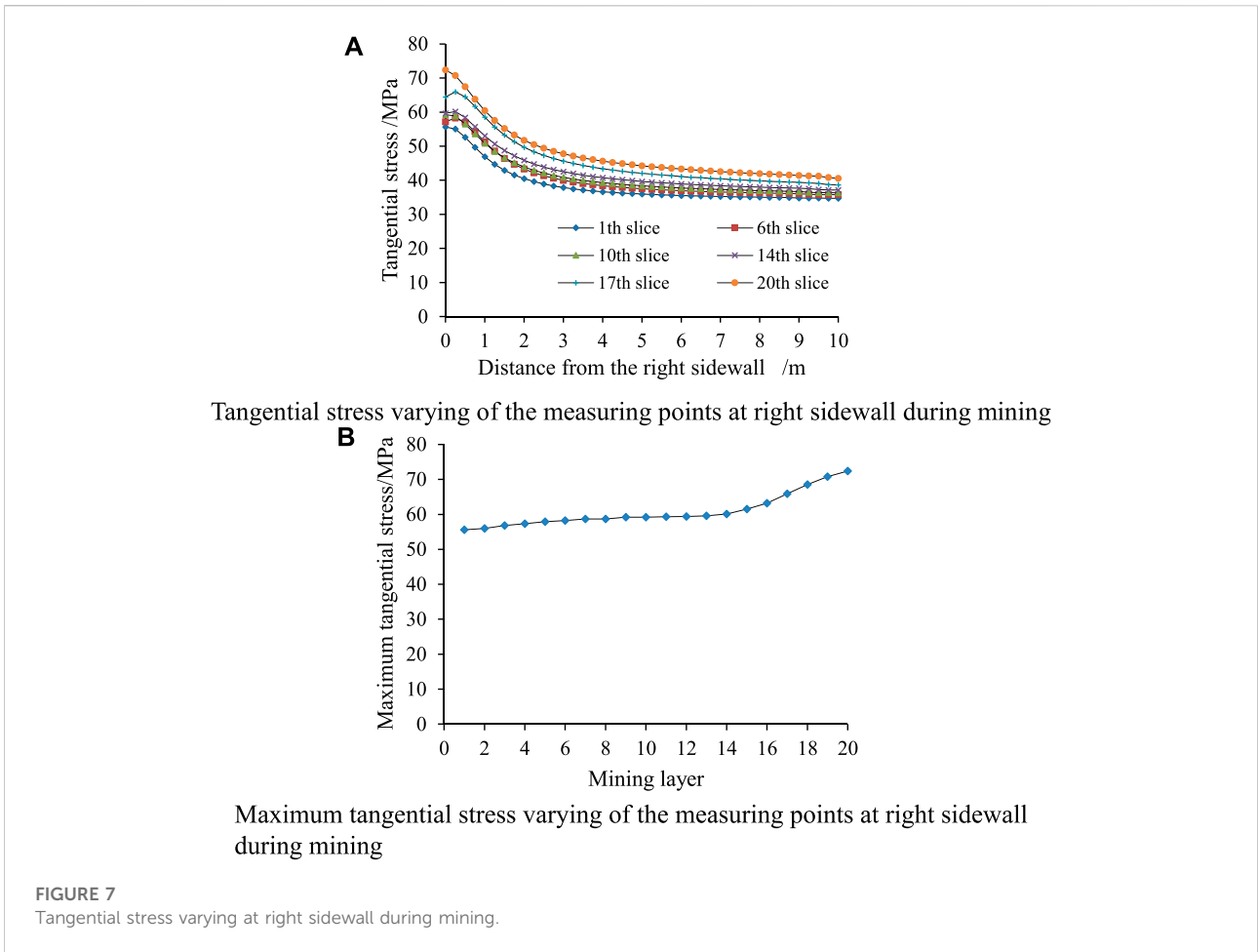


the ramp surrounding rock were not significantly developed and damaged. Therefore, Figure 9 only shows the detection results when mining the ore body above the 14th layer in the 13# stope.

Comprehensive analysis method

To analyze the failure evolution process of surrounding rock of the 13# stope ramp under the mining influence, a comprehensive analysis method combining field investigation,

numerical analysis and borehole detection was proposed (see Figure 5). In the field investigation, the failure characteristics and occurrence mechanism of the ramp surrounding rock were mainly analyzed to provide detailed data for the establishment of the numerical calculation model and the location of the borehole detection. The numerical analysis was used to study the evolution law of the tangential stress of the ramp surrounding rock under the mining influence. Borehole detection recorded the fracture depth of the ramp surrounding rock when different layers were mined.



Analysis of stress-fracture evolution of the ramp surrounding rock under the mining influence

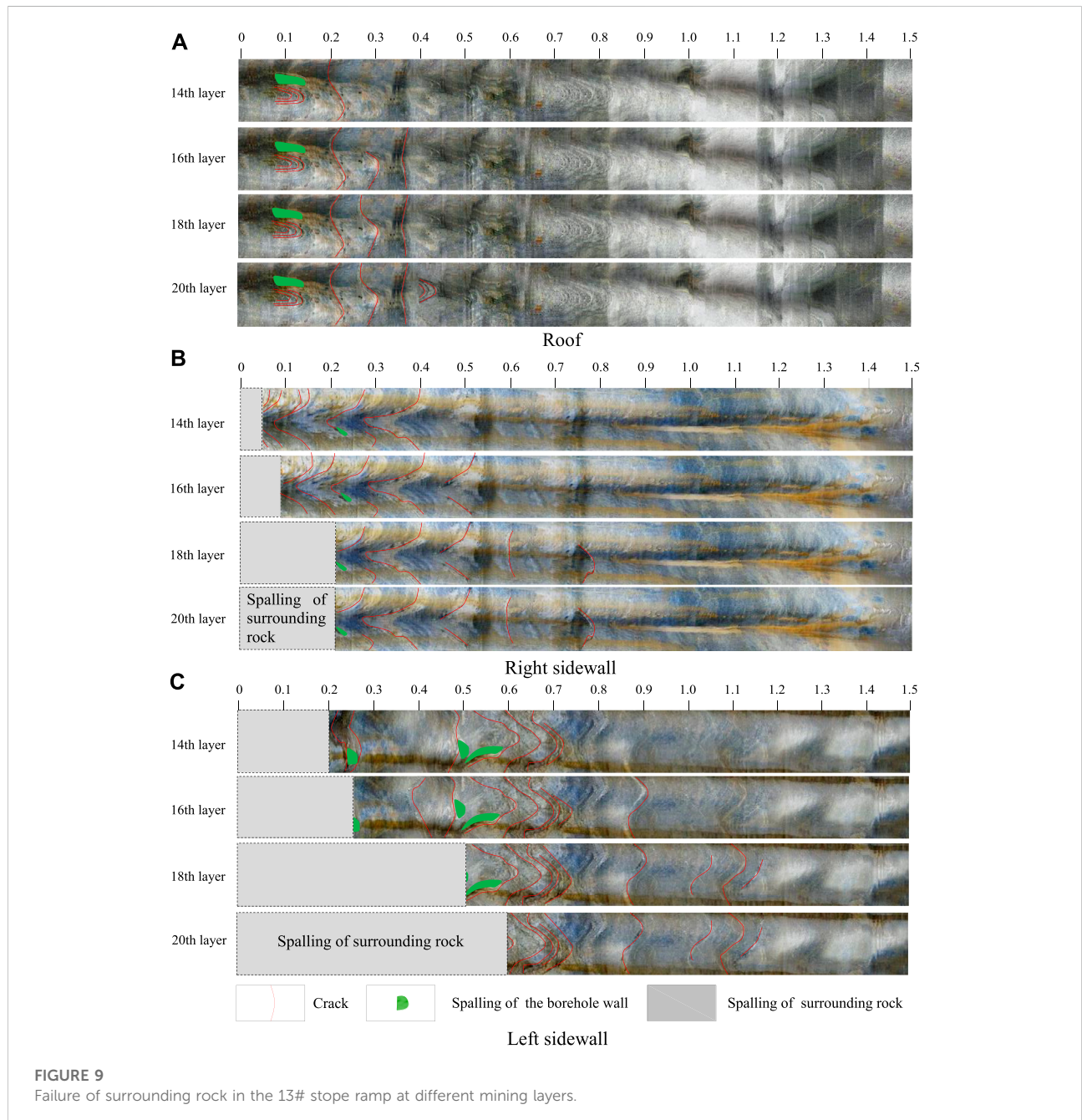
Analysis of tangential stress evolution of surrounding rock

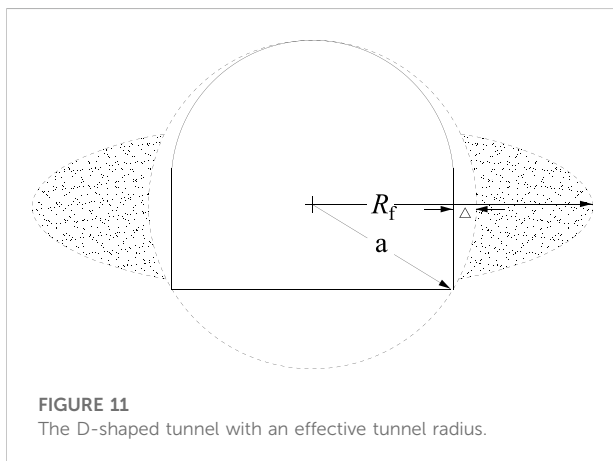
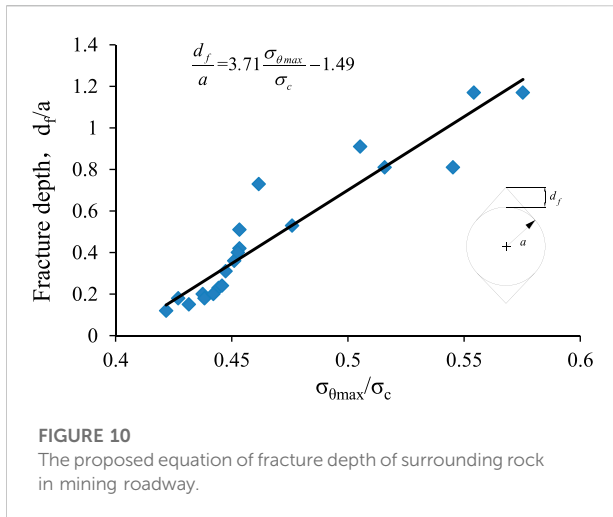
To analyze the evolution process of tangential stress of the surrounding rock under mining, measuring points were arranged every 0.2 m along the radial direction 10 m at the left, right and roof of the ramp, and the change of tangential stress at this point was monitored, as shown in Figures 6–8. For simplicity, the compressive stress was set as a positive value and the tensile stress as a negative value.

As shown in Figure 6A, with the increase of radial depth, the tangential stress value of the left sidewall first increases slightly, and then begins to decrease. When the depth is about twice the

TABLE 2 Comparative analysis of the maximum tangential stress and fracture depth of the ramp surrounding rock.

Position\Layered		2	4	6	8	10	12	14	16	18	20
Left sidewall	Maximum tangential stress/MPa	56.7	58.1	59.0	59.9	60.2	60.2	61.3	67.1	73.6	76.4
	Fracture depth/m	0.18	0.20	0.23	0.36	0.42	0.51	0.73	0.91	1.17	1.17
Right sidewall	Maximum tangential stress/MPa	56.0	57.3	58.2	58.7	59.2	59.4	60.1	63.2	68.5	72.4
	Fracture depth/m	0.12	0.15	0.18	0.21	0.24	0.32	0.40	0.53	0.81	0.81





roadway span from the left sidewall, the tangential stress value of this point tends to be stable. As can be seen from Figure 6B, when mining the ore body at the lower part of the ramp, the maximum tangential stress at the left sidewall increases slowly. When mining exceeds the level of the ramp (i.e., the ore body above the 14th layer), the maximum tangential stress increases rapidly,

and then tends to be stable. The maximum tangential stress is 76.4 MPa.

As shown in Figure 7, the tangential stress of the right sidewall has the same evolution law as that of the left sidewall. The difference is that the tangential stress of the right sidewall is slightly smaller than that of the left sidewall during the mining of the same layer. After mining the 20th layer, the maximum tangential stress peak value of the right sidewall is 72.4 MPa.

As shown in Figure 8, the tangential stress value is negative near the roof, and the roof is in the tensile stress zone. With the increase of radial depth, the tangential stress value of the roof changes from negative to positive, and then begins to decrease. When the depth is about twice the roadway span from the roof, the tangential stress value at this point tends to be stable. At the initial stage of mining, there is a tension zone on the ramp roof. When mining to the level near the ramp, the tension zone disappears. With the development of mining, the roof tension zone appears again. The maximum tangential stress value of the ramp surrounding rock during the whole mining process is listed in Table 2.

Analysis of evolution process of fracture depth of the ramp surrounding rock

The damage degree of surrounding rock is mainly judged by observing the development of cracks. The development range of cracks can be regarded as the fracture depth of the surrounding rock. The spalling fracture depth of surrounding rock generally refers to the depth of continuous failure or serious failure of rock mass (Wagner and Wiseman, 1980). Through the borehole detection of the ramp surrounding rock, the failure of surrounding rock in different periods of mining was obtained, as shown in Figure 9. The red line in the figure indicates the crack, the green area indicates the spalling of the borehole wall, and the gray area indicates the spalling of surrounding rock.

When mining the 14th layer, the mining layers are at the same level as the ramp. There are a few cracks on the inner wall of the 1# borehole (in the roof) from the orifice to the position of 0.24 m, and the cracks above the position of 0.24 m are not obvious. A large number of cracks are developed on the inner

TABLE 3 Comparative analysis of different methods for fracture depth of surrounding rock in engineering.

Cases\Methods	Numerical simulation/m	The proposed prediction equation	
		Depth d_f/m	Relative error/%
Underground transportation roadway of a mine in Canada Zhang and Mitri (2008)	3.50	3.22	8.0
Haulage roadway of Mufulira mine Kabwe and Bowa (2016)	0.83	1.01	21.7
Haulage roadway of Garson mine Abdellah et al. (2011)	3.81	3.42	10.2
Ore drawing roadway of Dongguashan copper mine Shu (2021)	2.50	2.21	11.6
Mean relative error/MRE			12.9

wall of the 2# borehole (in the right sidewall) from the orifice to the position of 0.4 m. The spalling with a thickness of 0.05 m in the orifice can be observed, and a small range of spalling appears on the borehole wall at the position of 0.22 m. The cracks above the position of 0.4 m are not developed. A large number of cracks are developed on the inner wall of the 3# borehole (in the left sidewall) from the orifice to the position of 0.73 m. The spalling with a thickness of 0.2 m in the orifice can be observed, and a small range of spalling appears on the borehole wall at 0.25, 0.5, and 0.55 m, respectively. The cracks above the position of 0.73 m are not obvious.

When the 16th layer is mined, the mining layers exceed the level of the ramp. New cracks appear in both sidewalls of the ramp and the roof borehole. Besides, the maximum depth of crack development in the 1# borehole (in the roof) is increased to 0.39 m, and the length of some original cracks is increased slightly. The maximum depth of the failure development in the 2# borehole (in the right sidewall) is increased to 0.53 m, and the depth of spalling failure is increased to 0.09 m. In the 3# borehole (on the left sidewall), the maximum depth of crack development in the 3# borehole is increased to 0.91 m, and the depth of spalling failure is increased to 0.26 m.

When the 18th layer is mined, no new cracks are found in the 1# borehole (in the roof), and only the length of some original cracks is slightly increased. Compared with the previous detection results, new cracks are generated in 2# and 3# boreholes (in the right and left sidewalls), and the crack development depth increases slowly, with the maximum depth of 0.81 and 1.17 m. The new spalling failure occurs in 2# and 3# boreholes (in right and left sidewalls), and the spalling fracture depth is 0.21 and 0.5 m, respectively.

When the 20th layer is mined, new cracks are produced again in the 1# borehole (in the roof), and the maximum depth of crack development increases to 0.44 m. There is no new crack in 2# borehole (in the right sidewall). No new cracks are found in the 3# borehole (in the left sidewall), but the spalling fracture depth is increased to 0.6 m. The fracture depth of the ramp surrounding rock during the whole mining process is summarized in Table 2.

Prediction of fracture depth of the roadway surrounding rock under the mining influence

Through the comprehensive analysis method of numerical analysis and borehole detection, the evolution process of the fracture depth of the surrounding rock under the mining influence is analyzed. As shown in Table 2, the fracture depth of the surrounding rock in the stope increases gradually with the increase of the maximum tangential stress of the surrounding rock, and the mining has a greater influence on the fracture depth of the left sidewall than the right sidewall. Combined with the failure mechanism of the ramp surrounding rock, it can be found

that the brittle failure of hard rock can be described by $\sigma_{0\max}/\sigma_c$. The linear fitting of the data (the maximum tangential stress and fracture depth in Table 2) is performed, then the equation of the fracture depth of the surrounding rock of the mining roadway can be obtained (see Figure 10) based on the equivalent radius (a) of the roadway and the ratio of the maximum tangential stress of surrounding rock to the uniaxial compressive strength of intact rock ($\sigma_{0\max}/\sigma_c$). When the analyzed roadway section is D-shaped, the effective radius of the roadway should be estimated (Figure 11). The estimated fracture depth of the roadway surrounding rock does not include the distance between the two sidewalls and the boundary of the equivalent circle (Δ). To verify the accuracy of the proposed equation, four engineering cases affected by mining are analyzed (Table 3), and their relative errors are calculated. Then the total error of all cases is predicted and averaged, and the average relative error is 12.9%. The calculation results of the proposed equation for the fracture depth of surrounding rock in mining roadways are in good agreement with the numerical analysis. It indicates that the proposed equation has great practicability and accuracy in predicting the fracture depth of surrounding rock in mining roadway, which can provide a basis for the support design of the engineering site.

Conclusion

Through the comprehensive analysis method of numerical analysis and borehole detection, the evolution process of surrounding rock fracture depth of deep mining ramp in Hongtoushan copper mine was studied. The following conclusions are obtained:

- (1) Numerical simulation is used to analyze the evolution characteristics of the maximum tangential stress of the surrounding rock under the mining influence, and the borehole detection analysis is carried out for the fracture depth of the surrounding rock under the mining influence. The results show that when mining the ore body at the lower part of the ramp, the maximum tangential stress and fracture depth of the two sidewalls of the ramp increase slowly. When mining exceeds the level of the ramp, the maximum tangential stress and fracture depth of the two sidewalls increases rapidly and reach the maximum value at the end of mining, and there is a positive correlation between the two values. In addition, the rock fracture depth of the left sidewall of the ramp is significantly greater than that of the right sidewall under the mining influence. Compared with the mining of the ore body below the ramp, the same level of mining has a greater impact on the fracture of surrounding rock.
- (2) The ratio of the maximum tangential stress of surrounding rock to the uniaxial compressive strength of intact rock

($\sigma_{\theta_{\max}}/\sigma_c$) and the equivalent radius (a) of the roadway are taken as parameters, and the equation of fracture depth of surrounding rock of the mining roadway is proposed. Through the engineering cases analysis, the proposed equation has good practicability and accuracy.

- (3) This study provides a basis for the stability analysis and support design of surrounding rock under the mining influence.

Data availability statement

The original contributions presented in the study are included in the article/supplementary material, further inquiries can be directed to the corresponding author.

Author contributions

HL conceived and designed the research. QZ performed the field investigations and experiments, presented the numerical simulation. HL and XZ wrote the original manuscript. BD and ZH participated in the data analysis and manuscript modification.

Funding

Key project of Natural Science research in Universities of Anhui Province (KJ 2021A0455), the State Key Laboratory of Safety and Health for Metal Mines (2021-JSKSSYS-02), Research

Start-up Fund for introduction of talents of Anhui University of Science and Technology, NSFC-Shandong Joint fund (Grant No. U1806208) and Research Funds for the Central Universities (N2001033).

Acknowledgments

Great appreciation goes to the editorial board and the reviewers of this paper.

Conflict of interest

Author ZH was employed by the company Zhuxianzhuang Coal Mine of Huaibei Mining (Group) Co., Ltd.

The remaining authors declare that the research was conducted in the absence of any commercial or financial relationships that could be construed as a potential conflict of interest.

Publisher's note

All claims expressed in this article are solely those of the authors and do not necessarily represent those of their affiliated organizations, or those of the publisher, the editors and the reviewers. Any product that may be evaluated in this article, or claim that may be made by its manufacturer, is not guaranteed or endorsed by the publisher.

References

- Abdellah, W., Mitri, H. S., and Thibodeau, D. (2011). Assessment of mine haulage drift safety using probabilistic methods of analysis[J]. *Procedia Eng.* 26, 2099–2111. doi:10.1016/j.proeng.2011.11.2412
- Abdellah, W., Raju, G. D., Mitri, H. S., and Thibodeau, D. (2014). Stability of underground mine development intersections during the life of a mine plan[J]. *Int. J. Rock Mech. Min. Sci.* 72, 173–181. doi:10.1016/j.ijrmms.2014.09.002
- Cai, M., and Kaiser, P. K. (2014). *In-situ* rock spalling strength near excavation boundaries[J]. *Rock Mech. rock Eng.* 47 (2), 659–675. doi:10.1007/s00603-013-0437-0
- Cai, M., and Lai, X. (2003). Monitoring and analysis of nonlinear dynamic damage of transport roadway supported by composite hard rock materials in linglong gold mine[J]. *Int. J. Minerals, Metallurgy Mater.* 10 (2), 10–15. doi:10.1109/5.771073
- Diederichs, M. S. (2007). The 2003 Canadian geotechnical colloquium: Mechanistic interpretation and practical application of damage and spalling prediction criteria for deep tunnelling[J]. *Can. Geotechnical J.* 44 (9), 1082–1116. doi:10.1139/t07-033
- Dowding, C. H., and Andersson, C. A. (1986). Potential for rock bursting and slabbing in deep caverns[J]. *Eng. Geol.* 22 (3), 265–279. doi:10.1016/0013-7952(86)90028-1
- Hoek, E., and Brown, E. T. (1980). *Underground excavation in rock*[M]. London: Instn Min. Metall, 1–76.
- Jia, H. S., Li, G. S., and Wand, L. Y. (2017). Characteristics of stress-field environment and roof falling mechanism of mining influenced roadway[J]. *J. Min. Saf. Eng.* 34 (04), 707–714. doi:10.13545/j.cnki.jmse.2017.04.015
- Kabwe, E., and Bowa, V. M. (2016). Determination of the appropriate geometry of footwall drifts using numerical analysis technique[J]. *Geotechnical Geol. Eng.* 34 (6), 1955–1969. doi:10.1007/s10706-016-0076-9
- Liu, W., Du, Y., and Liu, Y. (2019). Failure characteristics of floor mining-induced damage under deep different dip angles of coal seam[J]. *Geotechnical Geol. Eng.* 37 (2), 985–994. doi:10.1007/s10706-018-0666-9
- Martin, C. D., Kaiser, P. K., and McCreath, D. R. (1999). Hoek-Brown parameters for predicting the depth of brittle failure around tunnels[J]. *Can. Geotechnical J.* 36 (1), 136–151. doi:10.1139/t98-072
- Martin, C. D. (1993). The strength of massive Lac du Bonnet granite around underground openings. AvailableAt: <http://hdl.handle.net/1993/9785>.
- MartinChristiansson, C. D. R. (2009). Estimating the potential for spalling around a deep nuclear waste repository in crystalline rock[J]. *Int. J. Rock Mech. Min. Sci.* 46 (2), 219–228. doi:10.1016/j.ijrmms.2008.03.001
- Martini, C. D., Read, R. S., and Martino, J. B. (1997). Observations of brittle failure around a circular test tunnel[J]. *Int. J. Rock Mech. Min. Sci.* 34 (7), 1065–1073. doi:10.1016/s1365-1609(97)90200-8
- Ortlepp, W. D., and Stacey, T. R. (1994). Rockburst mechanisms in tunnels and shafts[J]. *Tunn. Undergr. Space Technol.* 9 (1), 59–65. doi:10.1016/0886-7798(94)90010-8
- Ortlepp, W. D. (2000). Observation of mining-induced faults in an intact rock mass at depth[J]. *Int. J. Rock Mech. Min. Sci.* 37 (1), 423–436. doi:10.1016/s1365-1609(99)00117-3
- Perras, M. A., and Diederichs, M. S. (2016). Predicting excavation damage zone depths in brittle rocks[J]. *J. Rock Mech. Geotechnical Eng.* 8 (1), 60–74. doi:10.1016/j.jrmge.2015.11.004
- Read, R. S. (2004). 20 years of excavation response studies at AECLA's Underground Research Laboratory[J]. *Int. J. Rock Mech. Min. Sci.* 41 (8), 1251–1275. doi:10.1016/j.ijrmms.2004.09.012

- Shu, J. B. (2021). Stability analysis and control techniques research on the surrounding rock of the ore-drawing roadway in dongguanshan copper mine. *Minerals* 11, 881. doi:10.3390/min11080881
- Waclawik, P., Kukutsch, R., and Konicek, P. (2017). Stress state monitoring in the surroundings of the roadway ahead of longwall mining [J]. *Procedia Eng.* 191, 560–567. doi:10.1016/j.proeng.2017.05.218
- Wagner, H., and Wiseman, N. (1980). The significance of rock fracturing in the design and support of mine excavations[J]. *Eng. Appl. Fract. Analysis* 1980, 399–407. doi:10.1016/b978-0-08-025437-1.50033-4
- Wang, C. H., Song, C. K., and Liu, L. P. (2012). Study of stress characteristics of brittle failures of rock around underground openings[J]. *Rock Soil Mech.* 33 (S1), 1–7. doi:10.16285/j.rsm.2012.s1.001
- Wang, H. W., Jiang, Y. D., and Xue, S. (2015). Assessment of excavation damaged zone around roadways under dynamic pressure induced by an active mining process. *Int. J. Rock Mech. Min. Sci.* 77, 265–277. doi:10.1016/j.ijrmms.2015.03.032
- Wei, W., Mitri, H., and Thibodeau, D. (2022). Stability of haulage drift in the dynamic mine environment. *Int. J. Rock Mech. Min. Sci.* 45, 973–986. doi:10.1016/j.ijrmms.2007.07.020
- Zhang, Y., and Mitri, H. S. (2008). Elastoplastic stability analysis of mine haulage drift in the vicinity of mined stopes [J]. *Int. J. Rock Mech. Min. Sci.* 45 (4), 574–593. doi:10.1016/j.ijrmms.2007.07.020
- Zhao, H., Ma, F., and Zhang, Y. (2013). Monitoring and mechanisms of ground deformation and ground fissures induced by cut-and-fill mining in the Jinchuan Mine 2, China[J]. *Environ. Earth Sci.* 68 (7), 1903–1911. doi:10.1007/s12665-012-1877-7
- Zhao, X., Li, H., and Zhang, S. (2019). Stability analyses and cable bolt support design for A deep large-span stope at the hongtoushan mine, China[J]. *Sustainability* 11 (21), 6134. doi:10.3390/su11216134
- Zheng, J. B., Wang, Q. Z., and Yang, S. (2015). Surround rock deformation and stability control technology of roadway influenced by repeating mining[J]. *Coal Min. Technol.* 3, 76–80. doi:10.13532/j.cnki.cn11-3677/td.2015.03.023